Prediction of Cutting Forces in Metal Cutting, Using the Finite Element Method, a Lagrangian Approach

Morten F. Villumsen[1], Torben G. Fauerholdt[2]

[1]Bang & Olufsen, Struer, Denmark
[2]Aalborg University, Department of Production, Aalborg, Denmark

Summary:

The purpose of this study is to introduce the first approach of metal cutting analysis. A Lagrangian based analysis is carried out using the LS-DYNA software. Simulated cutting forces are compared with forces measured by experiments. Series of sensitivity analyses were performed in order to evaluate the FEM (Finite Element Method) model. The model's sensitivity to changes of different parameters was examined. Experimental measuring of the cutting forces was performed with Kistler dynanometer type 9257BA.The numerical analysis was performed with the explicit finite element code LS-DYNA Ver. 971. rev. 7600.1224.
The chip formation was realistically modelled, but the output of forces from the analysis was overestimated when compared with forces measured during orthogonal cutting experiments. The cutting force F_x was overestimated by 104% and the thrust force F_z was overestimated by 60%. An analysis with better agreement between force output from analysis and measured forces has an unrealistic chip formation. In this analysis the cutting force F_x was underestimated by 2.1 % and the thrust force F_z was underestimated by 59.9 %, compared to forces measured during the experiments.

Keywords:

Metal cutting, Finite element method, Lagrangian, experimental measurement of cutting forces, numerical prediction of cutting forces, LS-DYNA

1   Introduction

Metal cutting is one of the most used production processes in the industry. The process is very flexible and can be used for production of parts with complex geometry and fine tolerances. Despite of the importance of this process, it is one of the production processes least examined. Furthermore, process parameters are still mainly chosen based on empirical knowledge. Experimental tests are costly and time demanding and even though material databases with a large number of material and tool combinations exist, the experimental tests show that these databases lose their relevance as new materials, tools and new and faster machines are developed. Thus, a better analysis of the cutting process is necessary in order to select cutting tools and process parameters.

1.1   Bang & Olufsen's Motivation

Since the 1960s Bang & Olufsen has used aluminium in their products. Aluminium is used as a design feature to express excellence in the luxury high-end audio and video products. The surface of the aluminium is very essential in expressing this. The processes used for the manufacturing of these aluminium surfaces are: grinding, polishing and metal cutting (milling and turning). All parts with

surfaces produced by these processes are subsequently anodized in order to obtain a scratch-resistant surface. These processes are among the core competencies at Bang & Olufsen.

The metal cutting processes such as milling and turning produce surfaces without any other after-treatment than the anodizing process, and these milled and turned surfaces are visible on the final Bang & Olufsen products. Therefore it is of extreme importance that surface errors are reduced to an absolute minimum.

The workpieces must be clamped and fixed during machining. Clamping of the workpieces in the machines became a vital issue lately. The clamping fixtures are very complex and very costly if all the demands on the surface are to be met. It is of high importance to minimize vibrations, surface and geometrical errors, and thereby reduce the production costs.

 In order to meet these demands and to continuously develop the metal cutting process, better modelling is necessary in order to predict cutting forces. At Bang & Olufsen we are working with steady improvement of the competencies within the field of metal cutting, and this work should contribute to a higher level of understanding the metal cutting process.

1.2   Analysis of Metal Cutting

Researchers have developed a large number of models for the metal cutting process during the last 60 years. As an example Kienzle [12] develops an empirical model based on a large number of experiments; Merchant [16], Armarego and Brown [10] and Oxley [14], develop analytical models. Within recent years mainly Finite Element Methods are used to simulate the metal cutting process, Massilimani [1], Raczy et al. [2] and Olovsson [19]. Improvements of manufacturing technologies such as metal cutting require better modelling and analysis. Numerical methods became recently an efficient tool for investigation of the complex phenomenon: metal cutting. The FE technique as a method for analysing metal cutting is a novel approach and can hopefully contribute to a higher level of understanding of this process. A more in-depth understanding is important for selection of cutting tools and process parameters.

However, it is a complex process which requires a metaphysic approach to handle the combined effects of material nonlinear behaviour, geometrical nonlinear behaviour and thermo mechanical effects.

1.3   Numerical Methods

Lagrangian and Euler techniques are typical approaches in the analysis of metal cutting as well as a combination of both - Arbitrary Lagrangian Euler (ALE). Furthermore, the Smooth Particle Hydrodynamics (SPH) method is used.

The main difference between Lagrangian and Euler methods is that the discrete mesh is coupled to the part and the material for the Lagrangian method; whereas the Euler method assumes that the material floats through a mesh controlled volume. In the ALE method the mesh does not need a coupling to the material, but can move arbitrarily. The mesh is moved during calculation to optimize the element form independently of the material deformation.

Smooth Particle Hydrodynamics (SPH) does not have a mesh as Lagrangian, Euler and ALE. Instead of a mesh the model is defined by a number of mesh-points (particles) with a field around them as shown in Fig. 1. The method was originally developed for problems in astrophysics, but it has been improved during the last decade. This method is used today in fluid and continuum mechanics, but full potential of the SPH method is not yet examined in-depth.
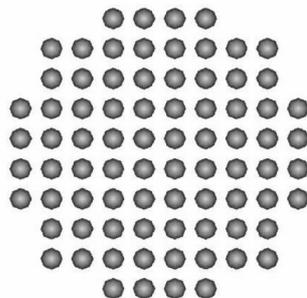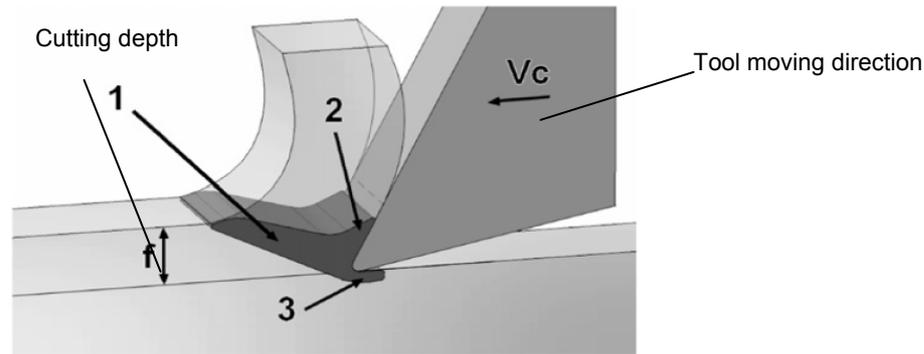

Fig. 1. Example of SPH mesh

Fig. 2. The three plastic zones in metal cutting, 1 The primary zone, 2 the secondary zone, 3 the tertiary zone, Limido et al. [3]
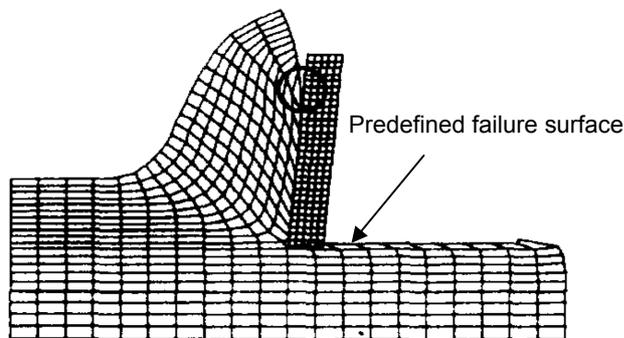

Fig. 3. Lagrangian element method with a predefined failure surface, Strenkowski and Carroll [11]

Strenkowski and Carroll [11] use the Lagrangian method with a model where a failure surface is predefined, see Fig. 3. In the cutting process both the material and the chip in the area of the tool tip yield, see Fig. 2. However, the fracture area at the tool tip is not well modelled using a failure surface. Therefore Lagrangian models without a predefined failure surface give a more realistic material flow. In these models the tool separates the material and the chip and then simulates the chip formation as it is shown in Fig. 2. Masillamani et al. [1] use a Lagrangian method in the FEM code LS-DYNA. The cutting temperature is examined in the models. Masillamani et al. achieve good agreement between temperatures from analysis and temperatures measured from tests.

Raczy et al. [2] use an Euler method to analyse the metal cutting process with the FEM code LS-DYNA. They achieve good agreement between predicted chip formation and measured chip formation. Cutting forces from the analysis are also compared with cutting forces measured from tests. The cutting force is examined for two material models: the hydrodynamics material model where the cutting force is overestimated by 13% and the Johnson-Cook material model where the cutting force is overestimated by 21%. For the definition of cutting forces see Fig. 4.
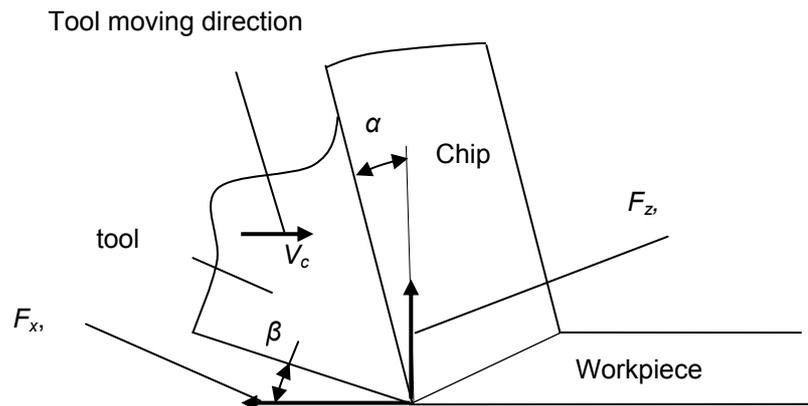
Fig. 4. Orthogonal cutting forces and angles, α: rake angle, β: relief angle, F_x
: The cutting force, F_z: The thrust force, V_c: cutting speed

The ALE method is used by Olovsson et al. [19] to analyse the metal cutting process where the goal is to predict chip formation. A few test simulations show promising results and the ALE formulation seems numerically robust.

Limido et al. [3] perform a 2D analysis with the SPH method in the FEM code LS-DYNA. Chip formation from analysis is compared to chip formation from tests and good agreement is reported. Moreover, cutting forces from experiments are also compared with cutting forces from analysis. The difference between the predicted and measured forces is 10% for the cutting force and 30% for the thrust force. These results are achieved using the Johnson-Cook material model, see Fig. 5.
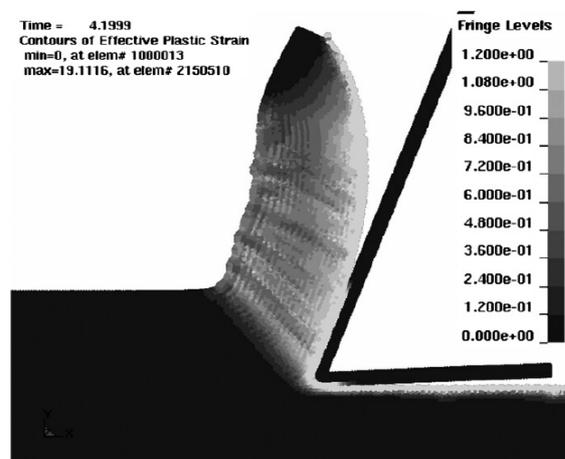

Fig. 5. Result from SPH analysis, showing the effective plastic strain, Limido et al. [3]

1.4   Material Models

Fang [5] performs sensitivity analyses of the flow stress of 18 different materials based on the Johnson-Cook material model. The effects of strain hardening, strain rate hardening and temperature softening on the material flow stress are examined. Fang concludes that strain-rate hardening is the least important factor governing the material flow stress, especially when machining aluminium alloys. In addition results for a few material types from the Johnson-Cook material model are compared with results from Oxley [14], Zerilli-Armstrong [17] and Maekawa's [18] material models.

Özel and Karpat [6] determine parameters for the Johnson-Cook material model by using "Co-Operative Swarm Optimization" (CPSO). CPSO is an optimization method here used to determine the material parameters by an inverse technique. The results are compared with other solutions, where material parameters are determined in a traditional way. Özel and Karpat achieve a better agreement

with CPSO results than the results determined in a traditional way, when data is compared with data from experimental tests. According to Özel and Karpat the method can also be used with other material models.

Sedeh et al. [7] extend Oxley's [14] analytical machining theory. Oxley's original theory treats only carbon steels. Sedeh et al. extend the theory to include also copper and aluminium. The theory for Qxley's original material model is compared with Johnson-Cook [9] and Maekawa [18] material models. Sedeh et al. conclude that Johnson-Cook and Maekawa models are better for predicting of cutting forces and temperature compared to experimentally achieved results than Oxley's original model. Jaspers [8] examines the Johnson-Cook and the Zerilli-Armstrong material models for both steel and aluminium. Jaspers compares the two material models and concludes that the mechanical material behaviour is so complex that it is not yet described accurately enough. It is insufficient to look only at flow stress as function of strain, stain rate and temperature. Jaspers concludes that the material models ought to be developed further, so that other parameters such as the material's micro-structure, like crystal orientation and size, as well as the solubility of the alloying elements are also taken into consideration.

1.4 Friction Models used in Analysis of Metal Cutting

Raczy et al. [2] and Sartkulvanich et al. [4] examine the area of friction modelling in metal cutting. The typical friction models used in analysis of metal cutting are coulomb friction and the shear friction model. The friction is in most cases a value, which is adapted to experimental data with the help of parameter variation. This is for instance carried out in the following ways: Raczy et al. [2] carry out a parameter variation on the coulomb-friction by comparing chip geometry from experiments and from FEM analysis. Sartkulvanich et al. [4] perform a sensitivity analysis of the friction by a parameter variation of the friction coefficient where cutting forces from experiments are compared with force output from FEM analysis. Limido et al. [3] use the SPH method in LS-DYNA and achieve to simulate the cutting forces with a 10 % deviation of the cutting force and a 30 % deviation of the thrust force compared to the experimental data. In the SPH method, when using SPH/SPH contact, the friction is modelled as particles interactions, and the friction parameter does not have to be defined. When using SPH/FEM coupling a friction parameter must be defined. Friction modelling in SPH must be studied in-depth but it offers a very interesting alternative to traditional definitions, Limido et al. [3].

2 FEM cutting model

In this section the model and sensitivity analyses for the model are described. The FEM cutting model is prepared for analysis in the FEM code LS-DYNA. The goal was to obtain a model with a calculation time as short as possible and which is able to predict the force output in agreement with forces measured from tests, and simultaneously predict a realistic chip formation. The FEM model used is a 3D solid model where the force output is examined in two directions; the cutting force direction and the thrust force direction. The analysis was performed with a constant speed of the tool in the *x* direction, as shown in Fig. 6. The tool has the same geometry as the tool used in the experiments. A comparison between the numerical analysis and the experiments is described in Section 4.

Based on the literature survey it is chosen to perform the analysis as described in the following text. Several assumptions were made in order to reduce the model size and the computation time, allowing the development of a useful method:
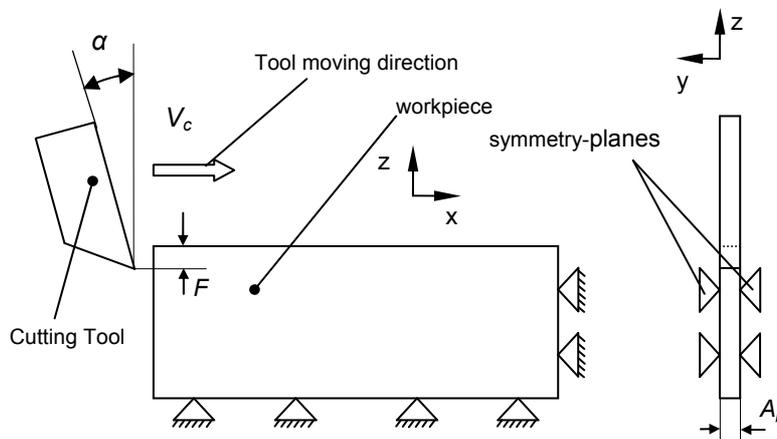

Fig. 6. The FEM model with constraints and nomenclature, V_c:cutting speed, F:cutting depth, A_p: cutting width, α : rake angle

The developed model, which is a 3D model, is implemented in an orthogonal cutting framework. In the analyses explicit time integration was used and Langrangian 8 nodes constants stress-solid elements were used *ELEMENT_SOLID: ELFORM 1.

The consistent unit system used in the analysis is (cm, g, µs).

The cutting tool is supposed to be perfectly sharp and rigid (no deformation), *MAT _020_RIGID" is used and the Rake angle on the cutting tool was α=0 degrees, see Fig. 6.

The workpiece was constrained as shown in Fig. 6 applied by *CONSTRAINED_GLOBAL. In the analyses the contact *CONTACT_ERODING_SURFACE_TO_SURFACE was used between cutting tool and workpiece.

The cutting parameters were: Cutting depth F = 0.234 mm, Cutting width Ap = 0.20 mm and Cutting speed V_c = 5m/s, see Fig. 6.

The cutting speed was imposed to the cutting tool by BOUNARY_ PRECRIBED_MOTION _RIGID" and *DEFINE CURVE.

The material model used for the workpiece was *098 MAT_SIMPLIFIED_JOHNSON_COOK in LS-DYNA.

If ε_p is the equivalent plastic strain, the von Mises flow stress σ according to the Johnson-Cook model, is given by Johnson and Cook [9]:

$$\sigma = (A + B \cdot \varepsilon_p^{\;n}) \cdot (1 + C \cdot \ln(\frac{\dot{\varepsilon}}{\dot{\varepsilon}_0})) \cdot \left(1 - \left(\frac{T - T_{room}}{T_{melt} - T_{room}}\right)^m\right) \qquad (1)$$

Where:

A is the material yield stress, B og n are strain hardening parameters, C is a strain rate parameter, $\dot{\varepsilon}$ is the plastic strain rate, $\dot{\varepsilon}_0$ is the calibration strain rate, m is a temperature coefficient, T is the real temperature, T_{room} is the room temperature and T_{melt} is the melting point of the specific alloy.

The Johnson-Cook material model takes into account the influence of strain, strain rate and thermal effects. In the used material model in LS-DYNA *098 MAT_SIMPLIFIED_JOHNSON_COOK the thermal effects and damage are ignored. The simplified material model was used since the necessary failure (damage) parameters for AL 6082-T6 in the material model *0015 MAT_JOHNSON_COOK were not found. Parameters for AL 6082-T6 used in these analyses are adapted from Jaspers [8]: A= 428.5 MPa, B=327.7 MPa, n=1.008, C=0.00747.

2.1   Sensitivity Analyses

Series of sensitivity analyses were performed in order to evaluate the model. A mutual comparison of the influence of the force output between two or more analyses in each specific sensitivity analysis was performed. The same tool geometry, chip depth and chip width was used in the models as in the experiments.

Sensitivity analyses must be performed on many parameters, but due to computation time this work is concentrated on the following:

The force output was examined when the following parameters were changed: mesh size, influence of mass-scaling, failure strain, (the effective plastic fracture strain) and friction between workpiece and tool.

2.1.1   Sensitivity Study of Mesh Size

In these analyses the mesh size influence on the force output was examined. The performed mesh analysis is an analysis of the mesh size influence on the force output fluctuations. The performed analysis is not a convergence study and in order to examine the mesh size influence on the force output, two different analyse sets were performed:

Mesh sensitivity analysis 1: Mesh size on the workpiece, where the tool had the same number of elements across the thickness, as the workpiece, see Fig. 7.

Mesh sensitivity analysis 2: Mesh size across the workpiece where the tool had more elements across the thickness than the workpiece, see Fig. 9.

The Mesh sizes on the workpieces examined in the analysis were in the top 0.075 cm.

2.1.2   Mesh Sensitivity Analysis 1

The main goal of this analysis was to examine mesh sizes on the tool and the workpiece influence on the force output fluctuations.The analyses were made under identical conditions, except the mesh size. They varied on element lengths of the workpiece with a factor 2 in the chip width, the chip depth

and in the moving direction of the tool, see Fig. 6. The dynamic friction coefficient FD and the static friction coefficient FS, were for these analyses both =0.2, the effective plastic failure strain PSFAIL = 2.5.
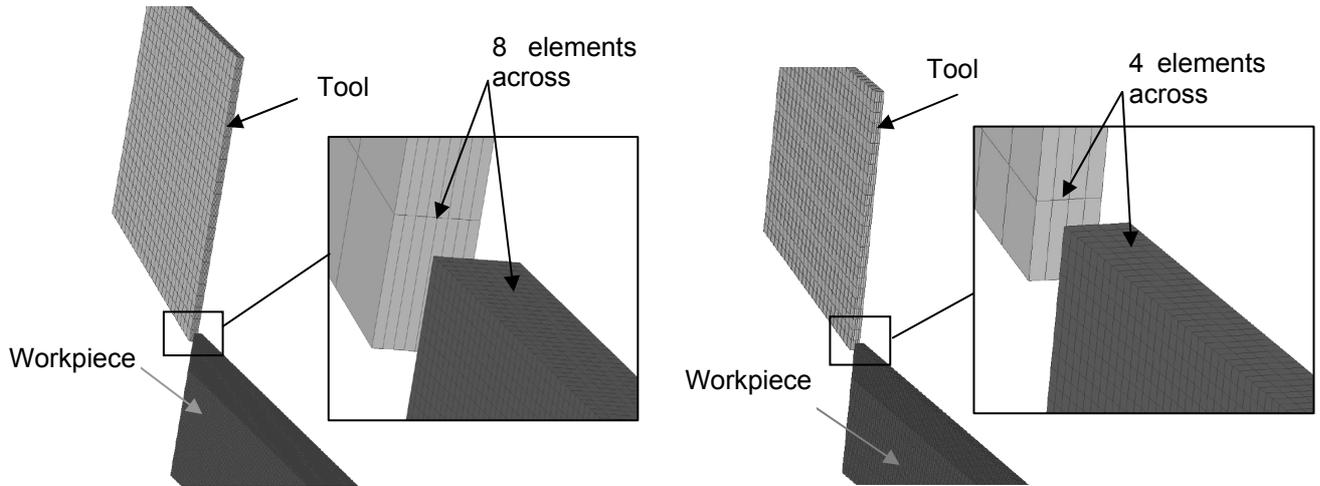

Fig. 7. Mesh size on the workpiece: left) analysis with fine mesh, right) analysis with coarse mesh

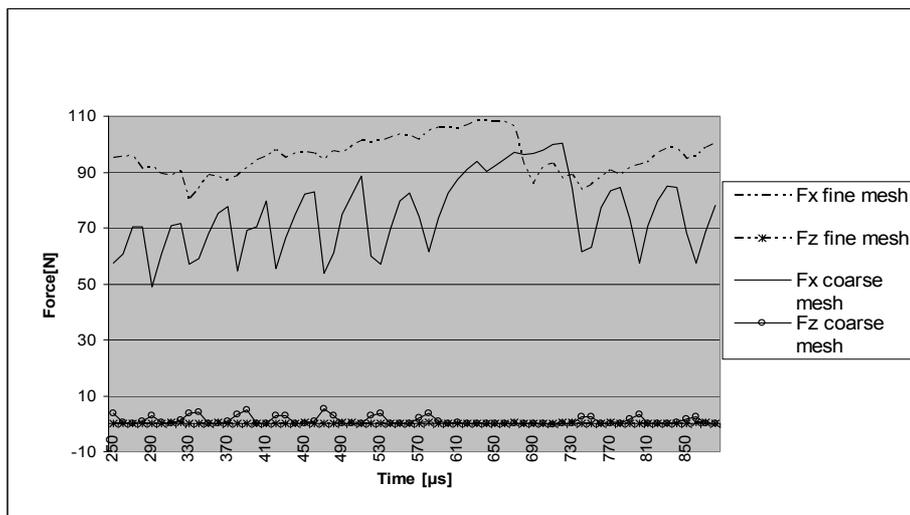The force output from the two analyses are compared in Fig. 8

Fig. 8. The simulated forces, the cutting force F_x and the thrust force F_z, for analysis with fine mesh and analysis with coarse mesh, time interval 250 – 880 µs

As shown in Fig. 8 there is a smaller fluctuation in the force output from the analysis with fine mesh compared to the analysis with coarse mesh. From these analyses it can be concluded that it is necessary with a fine mesh on the workpiece to be able to simulate a force output without too large fluctuations. In the analysis there are distorted elements under the cutting tool and in the chip. The analysis with fine mesh has less distorted elements than the analysis with coarse mesh. It is concluded that as the analyses carried out in "mesh sensitivity analysis 1" the deletion of the eroding elements are the primary cause of the fluctuations in the force output.

2.1.3   Mesh Sensitivity Analysis 2

The purpose of this analysis was to examine if the force output fluctuations only are dependent on the mesh size on the workpiece. These analyses were made under identical conditions, except for the mesh size on the workpiece. Two analyses were performed: One analyses with four elements across and another with one element across the workpiece, see Fig. 9. In both analyses there were 16

elements across the tool, see Fig. 9. The dynamic friction Coefficient FD and the static friction Coefficient FS, were for these analyses both =0.2, the effective plastic failure strain PSFAIL = 1.35.
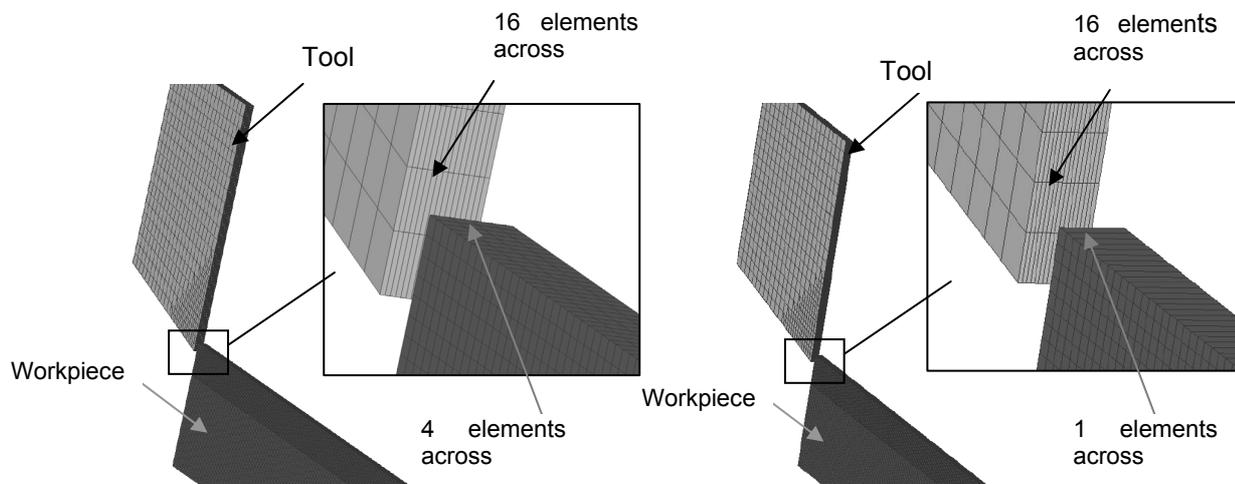

 Fig. 9. Mesh size on the workpiece: left) analysis with 4 elements across thickness, right) analysis with 1 element across the thickness. For both analyses the tool has 16 elements across the thickness

The force output for the analysis is compared in Fig. 10. As shown in Fig. 10 the fluctuation of the force output is smaller when there are several elements across the workpiece.
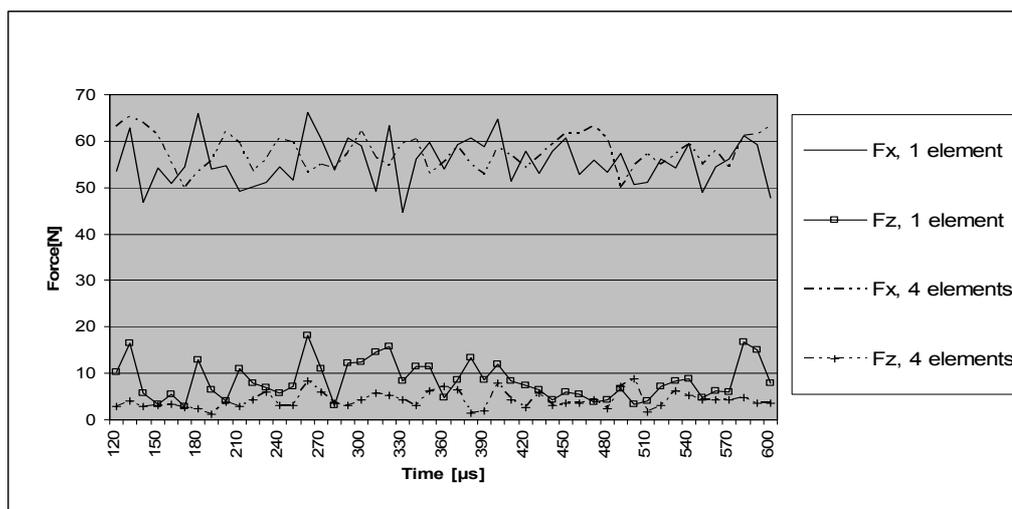

Fig. 10. Analysis 2: the simulated forces the cutting force Fx and the thrust force Fz, for analysis with one element analysis with four elements in the y-direction, time interval 120 – 600 µs

Judging from these analyses it can be concluded that a fine mesh across the workpiece is necessary in order to be able to simulate a force output without too large fluctuations. This is most distinct for the force output for the thrust forces F_z.

When the differences between the fluctuations of the force output from "Sensitivity analysis 1" are compared with the differences between fluctuations of the force output from "Sensitivity analysis 2", the fluctuations of the force output are minor when the mesh size on the tool is finer than on the workpiece. This is also stated by Bali [20]: *Rigid bodies should have a reasonably fine mesh, the node spacing on the contact surface of a rigid body should be no coarser than the mesh of any deformable part which comes into contact with the rigid body".* This can indicate that the mesh size in the *y*-direction of the tool reduces the fluctuations of the force output. This can be due to the fact that the

contact algorithm is sensitive to the mesh size on the tool. A solution, which can be used to avoid this problem, could be to use a VDA surface instead of a meshed part for the cutting tool.

2.1.4   *Sensitivity Analysis of the Effect of Mass Scaling*

Two analyses were carried out in order to examine mass scaling influence on the force output. The two analyses were identical except for that one was with mass scaling and one was without. The dynamic friction Coefficient FD and the static friction Coefficient FS, are for these analyses both =0.1 and the effective plastic failure strain PSFAIL = 2.0.
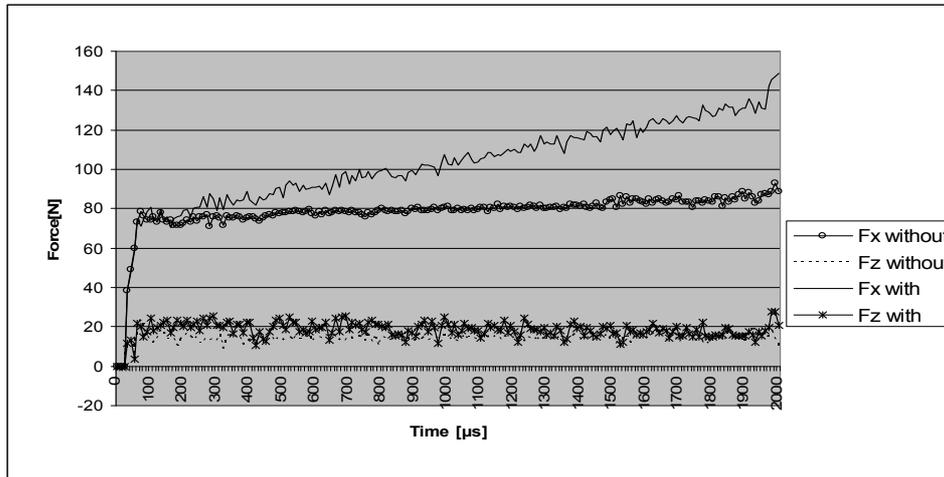

Fig. 11.   Simulated forces with and without mass scaling, for the cutting force F_x and for the thrust force F_z.

The force outputs for the two analyses are compared in Fig. 11. As shown in Fig. 11 the force output increased for the cutting force F_x for the analysis where the mass-scaling technique was used. For the analysis without mass-scaling the force output for the cutting force F_x was approximately constant. For the thrust force F_z both force output was approximately on a constant level, but the force output for the analysis with mass scaling was increasing. That is due to the fact that when using the mass-scaling technique, mass is moved to the elements that are exposed to a large plastic deformation. The chip contains elements exposed to large plastic deformation and thus the mass of the chip increases. When the mass of the chip increases the force output increases correspondingly and the force output increases. In the analysis with mass scaling a mass scale ratio 1.28 was used. At this mass condition the mass scaling technique can be used as an estimate by using a shorter analysis time, where the tool is in contact with the workpiece. The calculation time for the analysis is reduced from 161 hours without mass-scaling to 9 hours with mass-scaling.

2.1.5   *Sensitivity Study of the Effective Plastic Failure Strain Parameter*

Four analyses were carried out in order to examine the influence of the effective plastic failure strain parameter on the force output. It was chosen to examine the effect of the value of the effective plastic failure strain "PSFAIL" in *098 MAT_SIMPLIFIED_JOHNSON_COOK" in LS-DYNA. The four analyses were identical except for the value of the effective plastic failure strain. The dynamic friction coefficient FD and the static friction coefficient FS, were for these analyses both =0.1.

The force output for the four analyses was compared for the cutting forces F_x and the thrust forces F_z in Fig. 12.
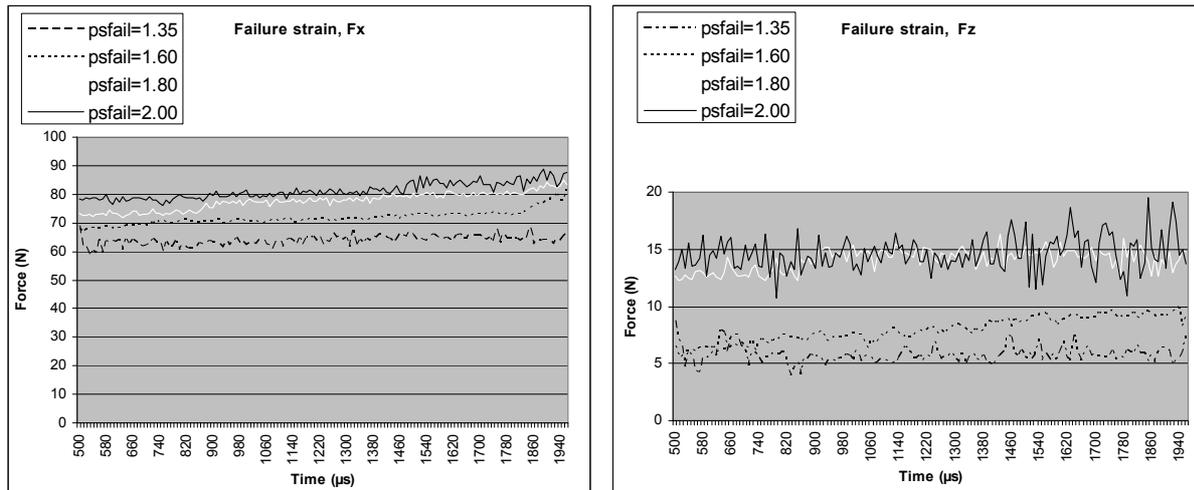
Fig. 12. The simulated cutting forces: left))the cutting force F_x, right)the thrust force F_z, where the forces have a steady state condition, for different values of the effective plastic failure strain "psfail", time interval 500 – 1960 µs
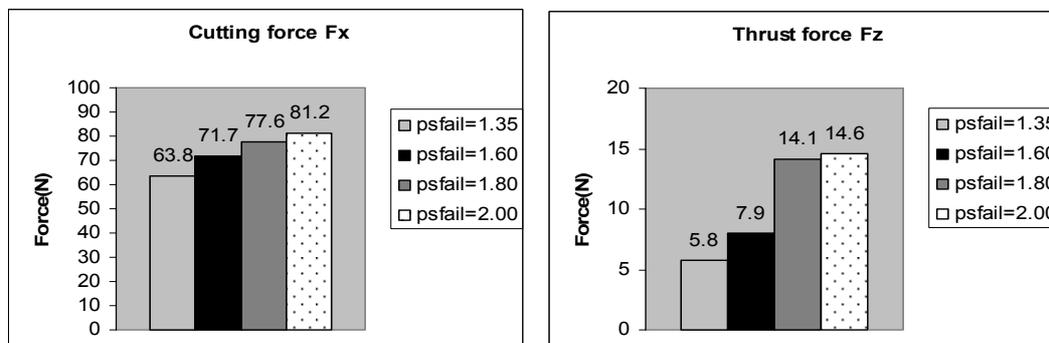

Fig. 13. Results of the four analyses: left) the cutting force F_x, right) the thrust force F_z, the values are average values

The largest fluctuations are in the force output for the thrust force F_z. In Fig. 13 the average values from Fig. 12 are compared.

As shown in Fig. 13 the force output for the cutting force F_x increases approximately proportionally with the failure strain "psfail". The force output for the thrust force F_z is not as proportional as in the cutting force's case. This is probably related to friction between tool and workpiece, this issue is dealt with in the next section.

2.1.6 Analysis of Friction between Workpiece and Tool

In order to examine the influence of friction on the force output, two analyses were carried out. These analyses were identical except for the values of the static friction coefficient *FS* and the dynamic friction coefficient *FD* in LS-DYNA. The static friction coefficient *FS* and the dynamic friction coefficient *FD* are in the following section named *µ* and no distinction will be made between the static and dynamic friction coefficient. The force output for the two analyses were compared, for the cutting forces F_x and the thrust forces F_z in Fig. 14 where the forces have a steady state condition. In order to reduce computation time both analyses were performed by using the mass scaling technique. As earlier described, this is the reason why the force curves have an increasing tendency. Since the conditions for both analyses were the same, a comparison is acceptable here.
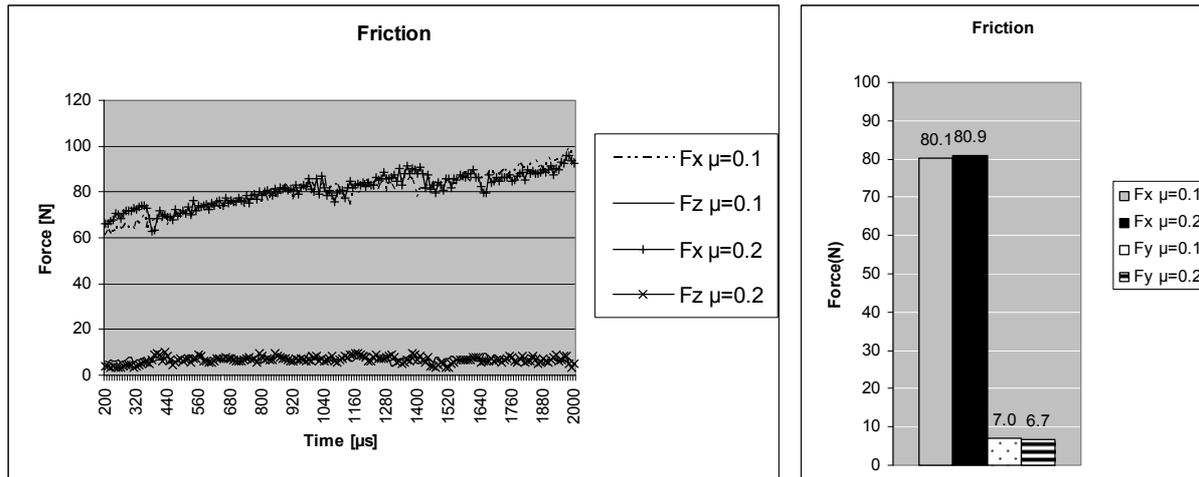
Fig. 14. The simulated forces where the forces have a steady state, for different values of the friction coefficient" µ", time interval 500 – 2000 µs. Left) Force output, right) average values of the forces

As shown in Fig. 14 the difference between the force output for the analysis with friction coefficient μ=0.1 and μ=0.2 is very small. For the cutting force F_x's case the force output is highest at a friction coefficient $\mu = 0.2$, while it in the thrust force F_z's case the force output is lower. This is opposite of what could be expected because the force output would be higher at a friction coefficient $\mu = 0.2$ for both the cutting force and the thrust force. Therefore it is obvious that this method does not model friction behaviour well.

3 Experimental Measuring of the Cutting Forces

In order to compare the force output from the numerical analysis and the actual cutting forces, it was necessary to carry out a number of experiments where the cutting forces were measured. The FEM model was a 3D solid model as earlier described, where the force output was examined in two directions: the cutting force direction F_x and the thrust force direction F_z. An often applied method to approach the conditions for orthogonal cutting is performed by machining the end of a thin-walled tube. Thus these FEM calculations can be compared with orthogonal cutting with good agreement. This method is used by Merchant [16], Armarego and Brown [10], Oxley [14], Stephenson and Agapiou [15] and Bissacco [13]. An example of this is shown in Fig. 15.
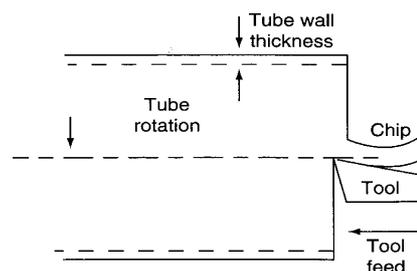

Fig. 15. End turning of a thin-walled tube to approach the conditions for orthogonal cutting, Stephenson and Agapiou [15]

3.1   Test Setup

The test setup in the lathe is shown in Fig. 16, the cutting tool engages with the end of the specimen. Force acquisition was started a few seconds before the beginning of the engagement and was stopped at the end of the test run. The experiments were carried out without use of cooling and lubrication.

Furthermore, the experiments were carried out with the following setup parameters: cutting speed V_c = 300 m/min, feed (chip depth) F= 0.234 mm/rev, chip width (the wall thickness on the specimen) A_a=
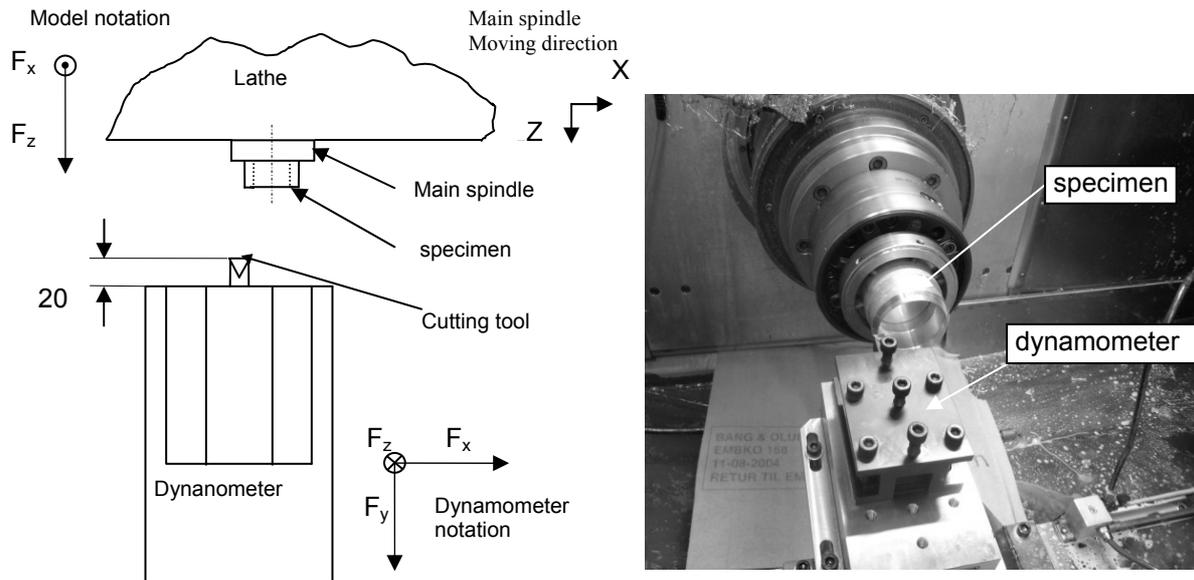

Fig. 16. The test setup, left) schematic drawing of the test setup in the Lathe, right) picture of test setup in the Lathe

0.2 mm and average diameter of the tube d_m = 65 mm. The specimen was an extruded aluminium profile, Material EN AW 6082 T6. The cutting forces were measured with a Kistler dynamometer type 9257BA and data from the measuring was stored in a PC. The Dynamometer was mounted on a console in the machine.

The main spindle gives the movement in the machine *x* and *z* directions, as shown in Fig. 16. Please note the different coordinate systems for the lathe, the dynamometer and the model.

In order to satisfy statistical demands, the experimental settings were made with five repetitions of each measure-cycle. The measured cutting forces, which were to be compared with the force output from the numerical analysis, were in this case taken when the measured force became a steady state condition, see Fig. 17.
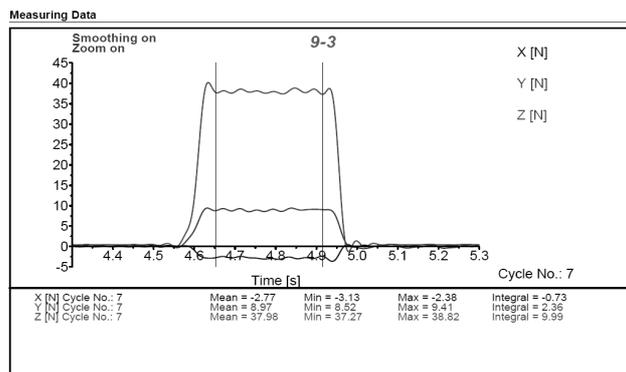

Fig. 17. Typical measure-cycle, steady state condition is between the two vertically lines.

When the measured raw-data was filtered, the average value was calculated for the time region between the two vertically lines, see Fig. 17, where the cutting force was in a steady state condition. Each of these average values represents a measure-value. The five repetitions of the measured forces from the experiment are shown in Table 1 .

The average value of the five measured values was calculated in two directions, the cutting force direction F_x and the thrust force direction F_z. The measured cutting forces were compared with force output from the analysis.

Test no.	Vc (cutting speed)	F(cutting depth)	Aa (chip width)	1 Fz1	1 Fx1	2 Fz2	2 Fx2	3 Fz3	3 Fx3	4 Fz4	4 Fx4	5 Fz5	5 Fx5	average values Fz	average values Fx
	m/min	mm/rev	mm	N	N	N	N	N	N	N	N	N	N	N	N
9 3	300	0.234	0.2	10.29	41.78	9.15	39.34	9.16	38.99	8.76	38.1	8.72	37.79	9.22	39.20

Table 1.   The test settings and the measured cutting forces

Measured cutting force F_x = 39.2 N, measured thrust force F_z = 9.2 N.

4 Comparison between Experiments and Analysis

In this section the analysis is presented which predicted the best agreement between force output from analysis and force output measured from experiments, at the same time as a realistic chip formation could be found. In this analysis the effective plastic failure strain was *PSFAIL*= 2.00 and the static friction coefficient *FS* and the static friction coefficient *FD* both =0.1. The effective plastic failure strain was adapted at a parameter variation in order to predict a realistic chip formation. The mesh size is shown in Fig. 18.
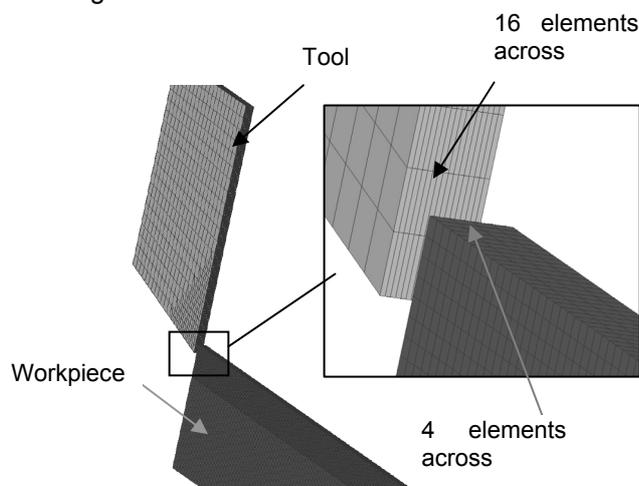

Fig. 18. Mesh size on the model , element length: across (cutting width) =0.05 mm, in the cutting depth =0.047 mm, and in the cutting direction =0.0476 mm

 As it is shown in Fig. 19, the chip formation is realistic. The tool separates the chip from the workpiece and the chip is continuously formed and curling in a natural manner.
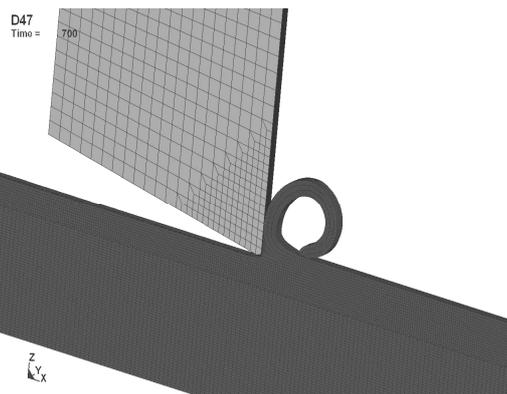

Fig. 19. Chip formation from the analysis

As shown in Fig. 20 the cutting force has a weak rising tendency while the thrust force F_z lies on an approximate constant level. The reason is that the chip is formed during the simulation and therefore the chip mass is increasing and the force output increases proportionally.
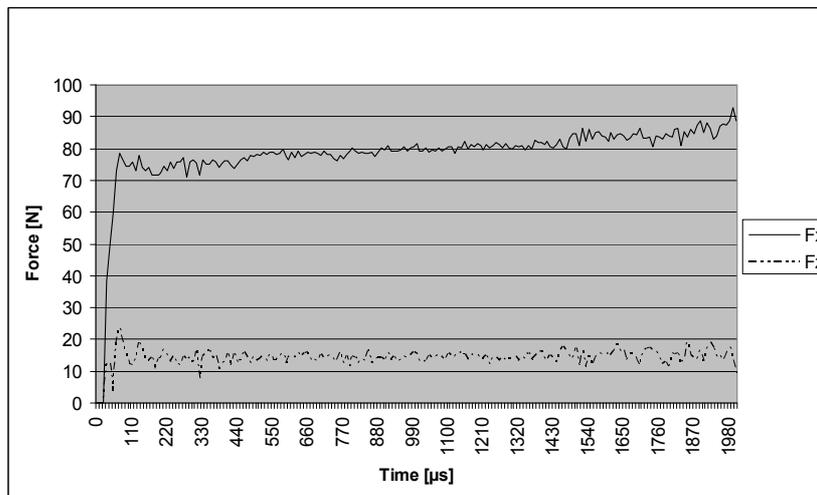

Fig. 20. Cutting forces from the analysis, Cutting force F_x and Thrust force F_z

When the average values from the analysis, where the force has a steady state condition, are compared with the measured forces from the experiments; the results shown in Fig. 21 are achieved. As shown in Fig. 21 there are deviations from the values of the cutting force F_x and the thrust force F_z. The cutting force F_x is overestimated by 104 % and the thrust force F_z is overestimated by 60 %, compared to forces measured from the experiments.

The failure criteria "PSFAIL" were too large in this analysis in order to predict the force output
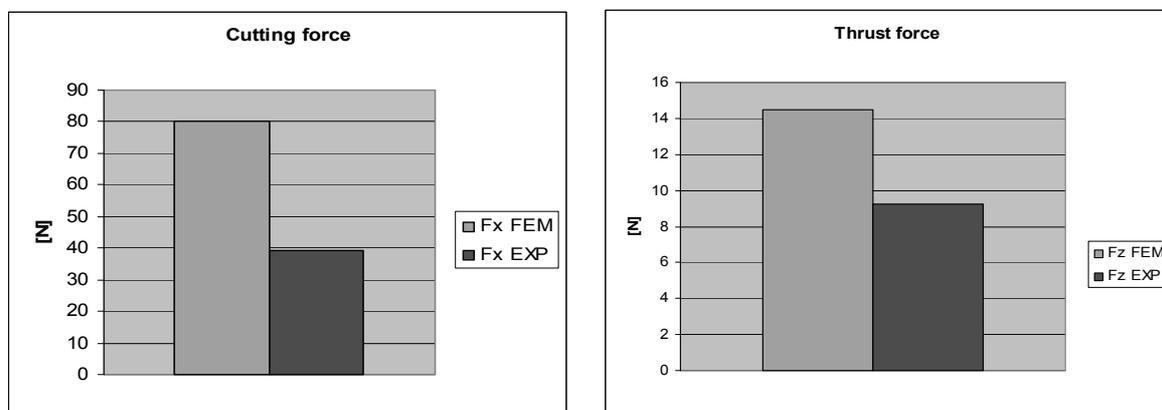

Fig. 21. Predicted forces from analysis of the cutting force F_x and the thrust force F_z compared to measured forces from experiment, the predicted values are average values from Fig. 20, time interval 100 – 2000 µs

according to cutting forces measured from experiments. The plastic failure strain "PSFAIL" is in this analysis adapted at a parameter variation, since the necessary parameter for the material used in this project was not found. The plastic failure strain has a significant influence on how well the force output and the chip formation can be simulated. By reducing the failure criteria to a smaller value the force output would be reduced, but the analysis of the chip formation would be less realistic. An example of an analysis with better agreement between force output from analysis and measured forces is shown in Fig. 22.
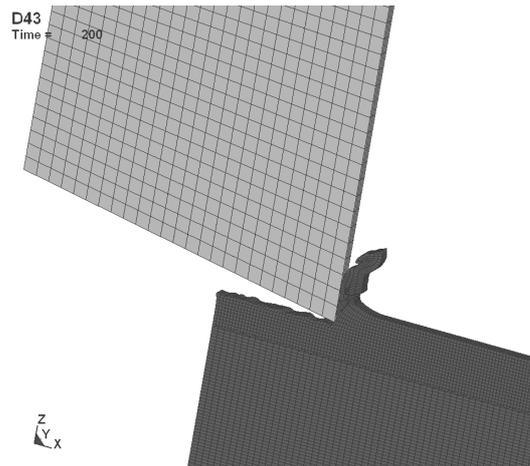
Fig. 22. Chip formation from analysis with"PSFAIL" =1.35

In this analysis the effective plastic failure strain is "PSFAIL"= 1.35 and the static friction coefficient "FS" and the dynamic friction coefficient "FD" both =0.2. The cutting force F_x is underestimated by 2.1 % and the thrust force F_z is underestimated by 59.9 %, compared to forces measured from the experiments.
It seems that it is possible to achieve a better analysis with finer mesh on the workpiece. When the elements are smaller, the influence by deletion of the eroding elements also has a minor influence on the force output fluctuations.
The analysis indicated a tendency to distorted elements primary in the area where the tool separates the chip and workpiece. The distorted elements can result in inaccuracies in the analysis. This problem can be minimized using an adaptive re-meshing technique where the mesh automatically is refined to those elements which are exposed to large deformation. A disadvantage of using adaptive re-meshing is that the method is very processor demanding which results in longer computation time. Another solution is to use the Smooth Particle Hydrodynamics (SPH) method instead of a mesh based method. The SPH method easily handles large strains that occur in the metal cutting process. The SPH method also handles the separation of chip/workpiece in a more natural manner than the Lagrangian FE model. In the SPH method it is not necessary to use a fracture model; the separation of the particles is implemented in the SPH method.

5 Conclusion

In this work series of sensitivity analyses were performed, the following parameters were examined: The influence of the mesh size on the force output fluctuations, Mass scaling influence on the force output, the friction influence on the force output and the failure criteria "PSFAIL's" influence on the force output.
The sensitivity analysis showed that a fine mesh on the work piece and tool is necessary in order to simulate a force output without too large fluctuations. Frictional behaviour is not very well predicted, the difference between the force output for friction coefficient μ=0.1 and μ=0.2 is insignificant and, therefore, it is not possible to make an unambiguous conclusion based on this analysis.
When using the mass scaling technique with a mass scaling ratio =1.28, mass scaling can be used as an estimate when the cutting length in the analysis is reduced.
The force output increases both for the cutting force and for the thrust force when the value of the effective plastic failure strain is increasing.

The analysis which predicted the best agreement between force output from analysis and force output measured from experiments, and, at the same time, predicted a realistic chip formation was found. The cutting force and the thrust force were predicted and compared with forces measured during the experiments. The cutting force F_x was overestimated by 104% and the thrust force F_z was overestimated by 60%.
By reducing the failure criteria to a smaller value the force output would be reduced, but the chip formation would be less realistic. An analysis with better agreement between force output from analysis and measured forces has an unrealistic chip formation. In the analysis the cutting force F_x is underestimated by 2.1 % and the thrust force F_z is underestimated by 59.9 %, compared to forces measured during the experiments.

Overall, a conclusion can be made that it was possible to improve the analysis of the force output. The chip formation was simulated realistically, but the estimate of the force output was too large.

Future work:
Future work will be concentrated on exploring the possibilities in simulation of metal cutting using Smooth Particle Hydrodynamics. The SPH method easily handles large strains that occur in the metal cutting process. The SPH method also handles the separation of chip/workpiece in a more natural manner than the Lagrangian FE model. In the SPH method it is not necessary to use a fracture model, the separation of the particles is implemented in the SPH method. Material data for the *MAT_JOHNSON_COOK material model in LS-DYNA are available and because the SPH method does not need fracture parameters, all material parameters are available.

6 References

1. Masillamani, D. and Chessa J., Determination of optimal cutting conditions in orthogonal metal cutting using LS-DYNA with design of experiments,2006, 8th International LS-DYNA users conference.

2. Raczy, A. et al., An Eulerian Finite Element Model of the metal cutting process, 2006, 8th International LS-DYNA users conference.

3. Limido, J. et al., SPH method applied to high speed cutting modelling, International Journal of Mechanical Sciences 49, 2007, pp. 898-908.

4. Sartkulvanich, P. et al., Effects of flow stress and friction models in finite element analysis of orthogonal cutting - a sensitivity analysis, Machining Science and technology 9, 2005, pp. 1-26.

5. Fang, N., A new Quantitative sensitivity analysis of the flow stress of 18 engineering materials in machining. Transactions of the ASME Vol. 127, 2005, pp. 192-196.

6. Özel, T. and Karpat, Y., Identification of constitutive material model parameters for high-strain rate cutting conditions using evolutionary computational algorithms, Materials and manufacturing processes 22, 2007, pp. 659-667

7. Sedeh, A. et al., Extension of Oxley's analysis of machining to use different material models, Transactions of ASME Vol. 125, 2003, pp. 656-666.

8. Jaspers, S., Metal cutting mechanics and material behaviour, Ph.D. T¨thesis, Technishe Universitet Eindhoven, 1999, ISBN 90-386-0950-7

9. Johnson, G.R. and Cook, W.H., A constitutive model and data for metals subjected to large strains, high strain rates and high temperatures, Proceedings of the 7th International symposium on ballistics, The Hague, The Nederlands,1983, pp. 541-547.

 10. Armarego, E.J.A. and Brown, R.H., The machining of Metals, Prentice-Hall ENGLEWOODS Cliffs,1969, New Jersey.

11. Strenkowski, J.S. and Carroll, J.T., Finite element model of orthogonal metal cutting with application to single point diamond turning, International Journal of Science. Vol. 30, No. 12, 1988, pp. 899-920.

12. Kienzle, O., Die Bestimmung von Kräften und Leistungen an spanenden Werkzeugen und Werkzeugmaschinen, Z-VDI 94,1952, pp. 299-302.

13. Bissacco, G., Surface Generation and Optimization in Micromilling, Ph.D. thesis, Technical University of Denmark, 2004, IPL246.04.

14. Oxley, P.L.B., Mechanics of machining, Ellis Horwood Limited, 1989.

15. Stephenson, D. and Agapiou, S., Metal Cutting Theory and practice, Taylor & Francis, 2006,ISBN 0-8247-5888-9

16. Merchant, M.E., Mechanics of metal cutting process. Journal of Applied Physics, 16.5, 1945, pp. 267-275 and pp. 318-324.

17. Zerilli, F.J. and Armstrong, R.W., Dislocation-mechanics-based constitutive relations for material dynamics calculations, Journal of Applied Physics, Vol. 61, 1987, pp. 1816-1825.

18. Maekawa, et al., Flow Stress of Low Carbon, Steel at High Temperature and Strain Rate Part 2, Flow Stress Under Variable Temperature and Variable Strain Rate, Bull. Jpn. Soc. Precis. Eng., 17, 1983, pp. 167–172.

19. Olovsson, L. et al., An ALE formulation for the solution of two dimensional metal cutting problems, Computer and structures 72, 1999, pp. 497-507.

20. Bala, S., Contact Modeling in LS-DYNA - Parts 1, 2, 3, and 4", Livermore Software Technology Corporation, 2001.